INTERPRETATION OF WHISTLER MODE CHORUS OBSERVATIONS WITH THE BACKWARD WAVE OSCILLATOR MODEL

U. Taubenschuss[*], A. G. Demekhov[†‡], and O. Santolík[*§]

Abstract

Observations of whistler–mode chorus made by the THEMIS spacecraft inside the equatorial chorus source region often exhibit the following peculiar features. Two groups of chorus elements are visible simultaneously which are approaching the spacecraft from two different directions: either along or against the direction of the ambient magnetic field. Furthermore, both groups are slightly shifted in frequency with respect to each other and elements are of different intensities. We interpret these features in the frame of the backward–wave oscillator theory by means of two exemplary events, yielding insight into the nonlinear generation mechanism and the specific source–observer geometry during the time of observation.

1 Introduction

Electromagnetic radiation of the whistler–mode, or R-mode, is a common phenomenon of planetary magnetospheres. In this paper we will focus on a special type, called chorus, which appears as discrete elements in a frequency–time spectrogram, often exhibiting positive (rising tones) or negative (falling tones) drift. Chorus has been extensively studied, especially in the vicinity of Earth, by past and present satellite missions [Taylor and Gurnett, 1968; Burton and Holzer, 1974; LeDocq et al., 1998; Santolík, 2008; Meredith et al., 2012; Li et al., 2013; 2016]. It is well accepted that the initial stage of generation can be explained by linear wave growth which is triggered by unstable electron populations via the first–order electron cyclotron resonance [Kennel and Petschek, 1966]. The relativistic first–order resonance condition between waves and electrons is given by

$$\omega - k_{\parallel}\, v_{\parallel} = \omega_{c,e}/\gamma \ . \tag{1}$$

[*] *Institute of Atmospheric Physics, Czech Academy of Sciences, Prague, Czech Republic*
[†] *Polar Geophysical Institute, Apatity, Russia*
[‡] *Institute of Applied Physics, Russian Academy of Sciences, Nizhny Novgorod, Russia*
[§] *Faculty of Mathematics and Physics, Charles University, Prague, Czech Republic*

Here, ω is the wave (angular) frequency, $k_\parallel$ is the wave vector's parallel component, $v_\parallel$ is the parallel component of the particle speed, $\omega_{c,e}$ is the electron cyclotron (angular) frequency, and the relativistic factor $\gamma = 1/\sqrt{1 - v^2/c^2}$, with c as the vacuum speed of light. Parallel components of $\mathbf{k}$ and $\mathbf{v}$ refer to the direction along the ambient quasi-static magnetic field $\mathbf{B}_0$. Since whistler–mode waves can only propagate at frequencies below the local electron cyclotron frequency, i.e. $\omega < \omega_{c,e}$, the product $k_\parallel\, v_\parallel$ must be negative so that Equation (1) can be fulfilled. This implies that resonance occurs between waves and particles propagating into opposite directions to each other, or, in other words, chorus is leaving the generation region in opposite direction to the motion of the resonant particles. Besides the linear growth phase, a complete description must involve also additional nonlinear wave–particle interactions, i.e. second and higher–order terms are retained in the appropriate interaction equations. This is necessary for explaining the spectral drift of chorus elements and for replicating observed high wave amplitudes, which often exceed a few hundred pT. Even if the exact nonlinear mechanism is still unclear, most theories have in common that the initial linear stage is triggered by an unstable electron population with a pronounced pitch angle anisotropy in the energy range of a few hundred eV to ∼100 keV. Anisotropic means that the particles' transverse velocities exceed their parallel velocities, i.e. $v_\perp/v_\parallel > 1$ (see e.g. Yue et al., 2016).

The concept of a backward–wave oscillator for explaining chorus generation was first proposed by Trakhtengerts [1995]. Backward–wave oscillators, or BWOs for short, have been known from laboratory experiments since the nineteen–fifties (see e.g. Johnson [1955]), and were mentioned by Brice [1963] when discussing triggered VLF emissions. A sharp electron beam stimulates the excitation of electromagnetic waves which travel at a group velocity directed opposite to the direction of electron motion. Even if sharp electron beams are absent in a magnetospheric plasma at the chorus generation region, Trakhtengerts et al. [1996] argued that sharp gradients in the velocity distribution function have a similar oscillatory effect. These gradients can be viewed as step-like deformations in phase-space which can be formed by noise–like emission, e.g. whistler–mode hiss, with a sharp upper frequency cutoff. In the frame of the BWO theory, $v_\parallel$ of the resonant electrons in Equation (1) is substituted by the velocity of the step–like feature, i.e. $v_\parallel = v_{step}$. Theoretical estimates show that such a step has not only a very small elevation (a few percent of the smooth part of the phase space density) but also rather small scales in energy and pitch angle, making it impossible even for modern particle detectors to resolve it [Trakhtengerts et al., 1996; 2004]. A recent study by Lyubchich et al. [2017] using Van Allen Probes data demonstrated that observed chorus growth rates cannot be replicated from the measured distribution functions, yielding further evidence for hidden fine structure such as steps. Despite this missing piece of evidence, the BWO theory makes a series of predictions which can be verified by observations, such as the occurrence of a chain of discrete chorus elements at a certain repetition rate, the link between the sweep rate of single elements and the plasma density, the frequency range as a function of distance to the source's center, as well as theoretical growth rates and wave amplitudes within the observed ranges [Trakhtengerts et al., 2007; Macúšová et al., 2010; Matsui et al., 2016; Demekhov et al., 2017]. In this paper, we will investigate the dependence of the observed chorus frequency and intensity on the source–observer geometry and combine it with a new aspect involving the direction of wave energy propagation. Instead of describing complex details of the

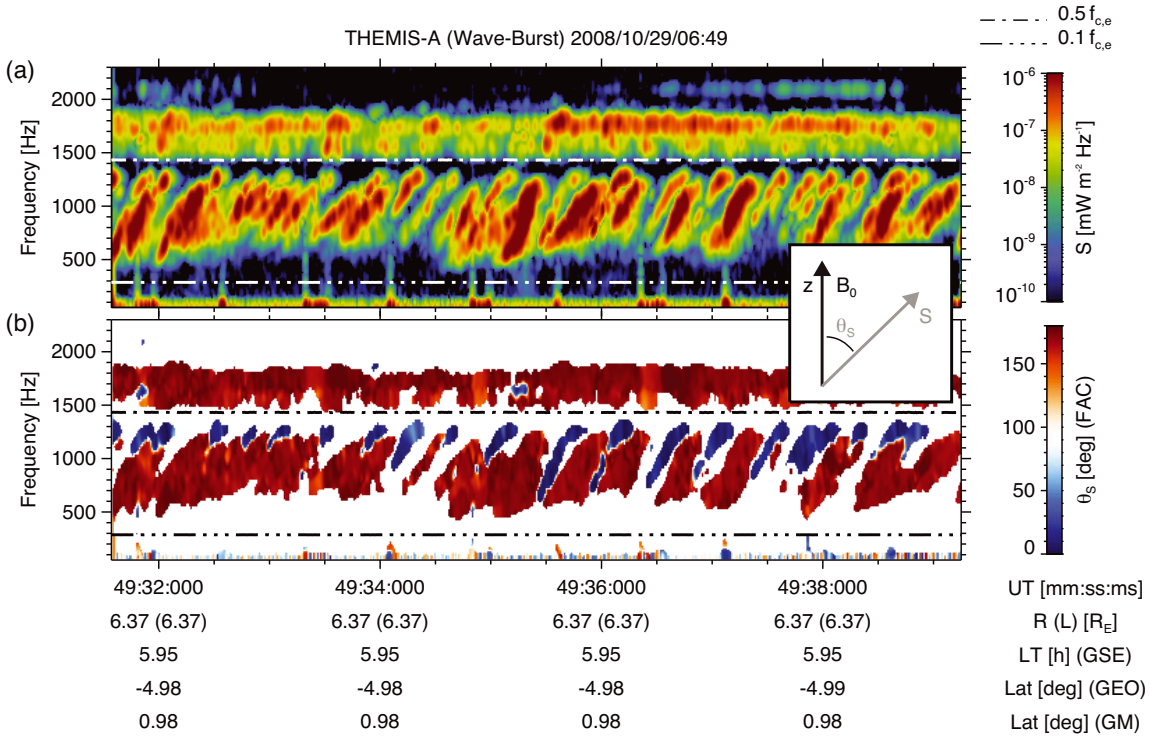

Figure 1: (a) Poynting flux S and (b) polar angle θ_S for chorus emission observed by THEMIS-A on October 29, 2008. The dashed–dotted line marks half of the local electron cyclotron frequency. Orbital coordinates of the spacecraft are given at the bottom. For weak $S < 10^{-8}\,\mathrm{mW\,m^{-2}\,Hz^{-1}}$, θ_S-values are shown in white color.

BWO theory, we will outline the general idea, and present chorus measurements made by the THEMIS (Time History of Events and Macroscale Interactions during Substorms) spacecraft [Angelopoulos, 2008] to support this idea. For detailed equations of the BWO theory we refer the reader to Demekhov et al. [2017].

2 THEMIS data

The THEMIS mission was launched in early 2007. It consists of five spacecraft on near–equatorial orbits around Earth, all carrying identical instruments. Three magnetic search coil magnetometers [Roux et al., 2008] and three electric antennas [Bonnell et al., 2008] can be operated in a "wave–burst" mode which samples magnetic and electric waveforms at a sampling rate of 8192 Hz. These measurements enable polarization analysis of whistler mode chorus with the necessary high time–frequency resolution. Waveforms are subject to spectral analysis yielding auto-correlation and cross-correlation products which are compiled to a complex spectral matrix. The spectral matrix is analyzed via singular value decomposition [Santolík et al., 2003]. Singular values and singular vectors contain the full information on the polarization of measured waves.

Figure 1 shows an example for a wave–burst mode snapshot taken by THEMIS-A in the middle magnetosphere (L-shell $\sim$ 6.37) close to the magnetic dipole equatorial plane

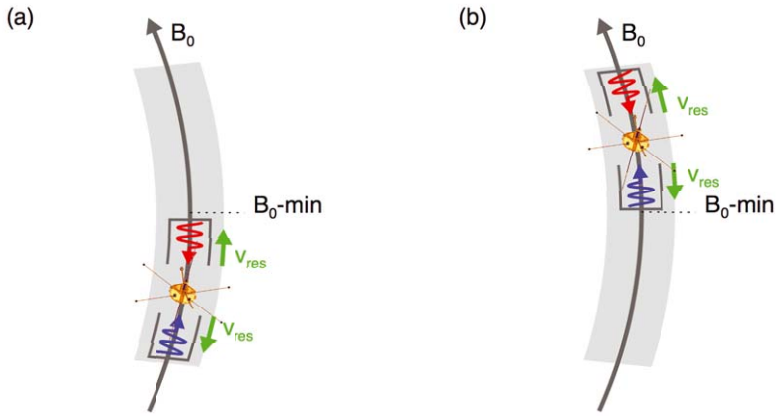

Figure 2: Simplified sketch of the source–observer geometry for two different scenarios: (a) THEMIS being south of the true magnetic equator (B_0-minimum) and (b) THEMIS being north of it. Two BWO interaction regions (BWO–IRs) surrounding THEMIS are drawn in each panel. The directions of wave propagation are indicated by blue and red wavy symbols. The parallel velocities of resonant electrons for each BWO–IR are indicated by green arrows.

($\mathrm{LAT_{GM}} \sim 1°$). These snapshots usually last for 8 s and cover a total frequency range of 0–4 kHz. Six cross-correlation products from electric and magnetic waveforms have been combined to calculate the Poynting vector **S** which describes the propagation of electromagnetic energy [Santolík et al., 2010]. **S** is displayed in terms of absolute value, i.e. Poynting flux (see Figure 1a), and polar direction angle θ_S (see Figure 1b) in the field-aligned coordinate system (FAC). This system has its z-axis aligned with the direction of the ambient magnetic field $\mathbf{B_0}$ (see also small insert in Figure 1).
Intense chorus is clearly visible between 500–2000 Hz. The ellipticity parameter (not shown here) confirms that the emission is right-hand polarized whistler–mode. A gap in intensity at 0.5 $f_{c,e}$ ($f_{c,e}$ is the local electron cyclotron frequency) splits the emission into a lower and an upper band. The lower band consists of a sequence of discrete elements with positive sweep rates, i.e. rising tones. A closer look at Figure 1b reveals that rising tones approach the spacecraft from two different directions: either along the direction of $\mathbf{B_0}$ ($\theta_S \sim 0°$; shown in blue) or against the direction of $\mathbf{B_0}$ ($\theta_S \sim 180°$; shown in red). A simultaneous visibility of both propagation directions is a strong indication for THEMIS-A being inside the chorus source region during the time of observation. Besides the opposite propagation directions, there are two more differences visible: first, there is a slight shift in frequency between elements approaching along and against $\mathbf{B_0}$, and second, elements approaching along $\mathbf{B_0}$ have a smaller Poynting flux. These differences in frequency and intensity in dependence on the direction of propagation can be explained by the BWO model for chorus generation.

3 Results

The BWO model makes specific predictions for observations inside the chorus source region. With the term "source region" we mean the total latitudinal range of an ac-

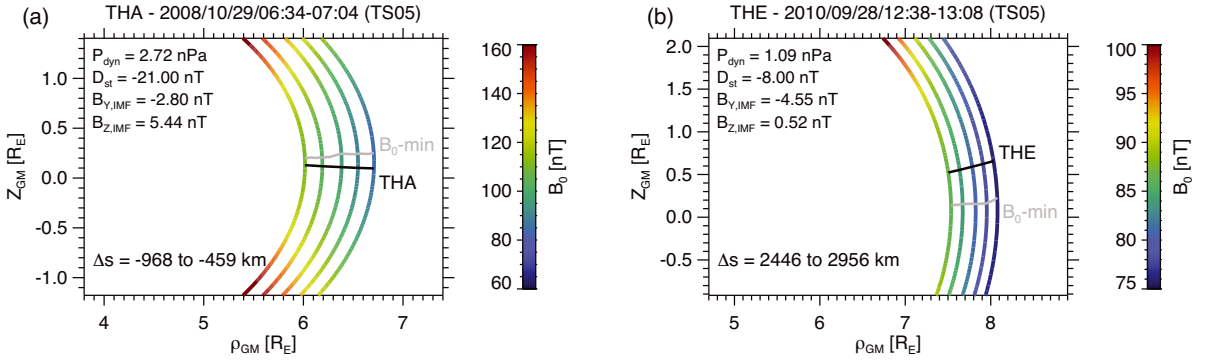

Figure 3: Magnetic field configuration in the meridional plane of the geomagnetic coordinate system, as derived from the TS05–model for the observations presented in (a) Figure 1 and (b) Figure 4. The magnetic field strength B_0 along the field lines is indicated in color. B_0-minima are connected with a gray solid line. The trajectory of the spacecraft is delineated by a black solid line. Solar wind input parameters for the center-time are listed as well: dynamic pressure (P_{dyn}), D_{st}-index, and y- and z-component of the interplanetary magnetic field (in GSM coordinates). The range of distances Δs along the field lines between the B_0-minimum and the position of THEMIS is given at the bottom.

tive magnetic flux tube along which energetic electrons can lead to nonlinear growth of whistler–mode waves. This region is confined to within ±6° around the true magnetic equator, i.e. around the B_0-minimum along the magnetic field line [LeDocq et al., 1998; Santolík et al., 2005; Taubenschuss et al., 2016]. It is highlighted by the elongated gray shaded area in Figure 2. Results from modeling, which will be presented elsewhere, show that an individual chorus element is generated inside a smaller subregion that is embedded inside the global source region. This generation region for a single element is called BWO interaction region (BWO–IR). It is indicated in Figure 2 by an open box containing a colored wavy symbol. A BWO–IR can stretch up to ∼2000 km along $\mathbf{B_0}$ [Trakhtengerts et al., 2007], but is limited to <100 km transverse to $\mathbf{B_0}$, i.e. to a few wavelengths [Santolík et al., 2004].
Statistical analyses have shown that chorus Poynting vectors remain quasi field-aligned during propagation away from the BWO–IR [Li et al., 2013; Taubenschuss et al., 2016], making it reasonable to assume that, if THEMIS is located inside the source region, the BWO–IR can be found along the magnetic field line which is penetrating the spacecraft.

Figure 2a provides an illustration for how to interpret the observation of THEMIS-A presented in Figure 1. According to the BWO theory, chorus elements being generated further away from the B_0-minimum and propagating towards it are at higher frequencies and also have weaker intensities if compared to similar elements being generated closer to the B_0-minimum. The elements propagating away from the B_0-minimum experience only slight changes in frequency. If we combine this information with the observed directions of Poynting vectors, the more distant BWO–IR to the B_0-minimum generates the blue elements from Figure 1b. Such a source–observer geometry is only possible if THEMIS-A is not only located within ±6° of the B_0-minimum, but also it has to be located south

of the B_0-minimum. Unfortunately, the exact position of the B_0-minimum cannot be derived from single spacecraft measurements because ∇B_0 is not known. Thus, we have to rely on a model for the external magnetic field. The geomagnetic dipole model yields $\mathrm{LAT_{GM}} = +0.98°$, i.e. THEMIS-A being north of the B_0-minimum (see coordinates at the bottom of Figure 1). However, a dipole field is just a crude approximation for the true field at radial distances beyond $6\,\mathrm{R_E}$ ($\mathrm{R_E}$ is the radius of Earth). Thus, for the time of measurement, we compute the magnetic field line through the position of THEMIS-A with the more accurate Tsyganenko–TS05 model [Tsyganenko and Sitnov, 2005]. It needs additional input parameters from the solar wind which are provided by the ACE and Wind satellites [Lepping et al., 1995; Lin et al., 1995; McComas et al., 1998; Smith et al., 1998]. The results from the TS05 model are presented in Figure 3a. Five field lines are plotted during an interval of 30 minutes around the time of measurement in Figure 1. The trajectory of THEMIS-A is indicated by a black solid line, which turns out to be south of the gray solid line which is connecting B_0-minima across field lines. At the central field line in Figure 3a, i.e. at the time of wave–burst measurement, THEMIS-A is indeed ∼860 km south of the B_0-minimum.

For comparison, we present another event observed by THEMIS-E on September 28, 2010. The spacecraft is again located close to the magnetic equatorial plane and observes chorus elements with two distinct directions for the Poynting vector. However, the situation seems to be reversed in comparison to the event from THEMIS-A. As can be seen in Figure 4, elements propagating against the direction of $\mathbf{B_0}$ (shown in red) are weaker and are shifted toward higher frequencies. The corresponding geometry between THEMIS-E and the two BWO–IRs is sketched in Figure 2b. Observations agree with the BWO theory only if THEMIS-E is located north of the B_0-minimum. As shown in Figure 3b, calculations with the TS05–model confirm that THEMIS-E is indeed ∼2750 km north of the B_0-minimum at the time of measurement.

4 Discussion and conclusions

We present two exemplary events from THEMIS-A and THEMIS-E of chorus observations made inside the equatorial source region. A simultaneous visibility of opposite propagation directions for chorus elements and differences in frequency and intensity can be explained with the backward–wave oscillator theory. This theory demands a certain source–observer geometry and specifies if the observer is positioned north or south of the true magnetic equator, i.e. the B_0-minimum along the field line. For both presented events, observations and BWO theory complement one another. In total we found 146 events of varying quality among THEMIS-A, THEMIS-D and THEMIS-E during the years 2008–2012. One of the next steps will be to investigate the best cases with numerical simulations. This will provide further insight into how the observable features (Poynting vector direction, shift in frequency, intensity variation) depend on other important parameters such as B_0-gradient and distance between BWO–IR and the observer along the field line, or the variation of the energetic electron distribution along the field line.
We finish with a brief reflection on alternative ways to interpret the observations. Agapitov et al. [2011] analyzed a similar event from THEMIS-A and concluded that chorus

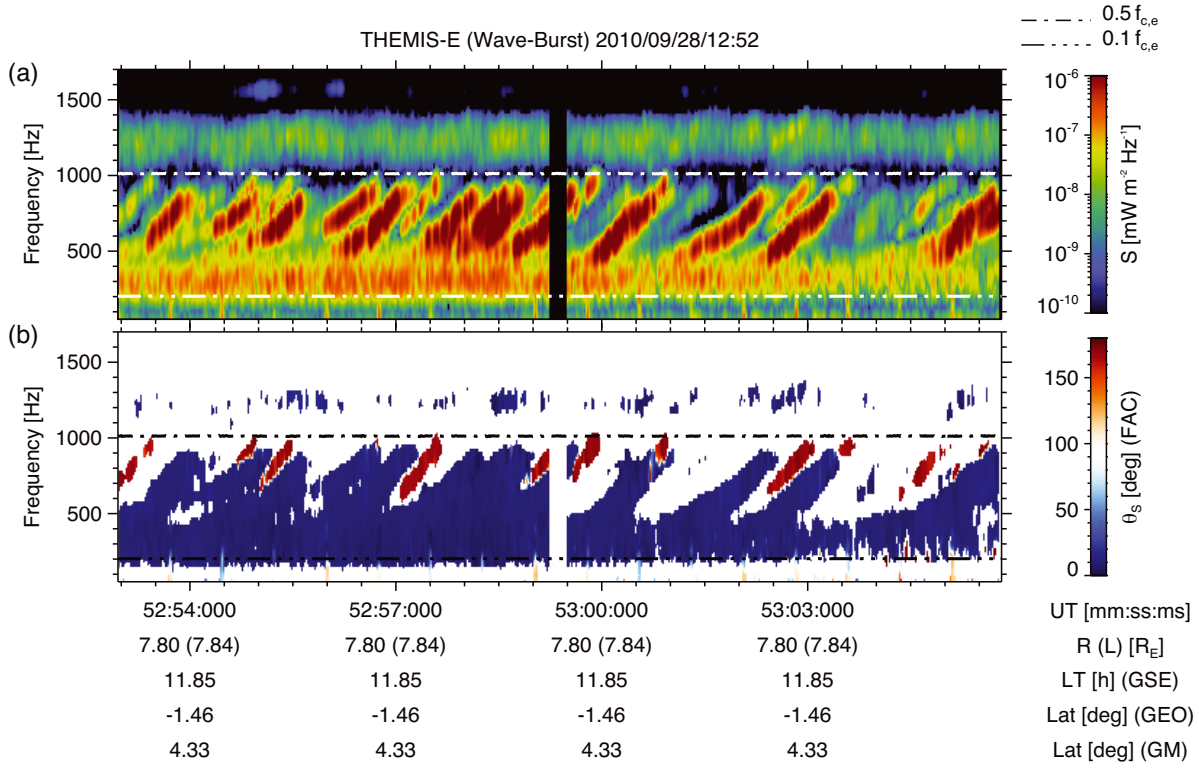

Figure 4: Chorus (a) Poynting flux S and (b) polar angle θ_S observed by THEMIS-E on September 28, 2010 (see also caption of Figure 1).

elements with slightly higher frequencies must have been generated at lower L-shells, from where they propagate toward the spacecraft via magnetospheric reflection at high magnetic latitudes (beyond 50°). Measured simultaneously with a locally generated group of elements in the equator can produce spectra such as shown in Figure 1 and Figure 4. A controversial aspect of this theory is that reflected chorus becomes significantly attenuated along the ray path, making it several orders of magnitude weaker than the locally measured chorus (see e.g. Parrot et al. [2004] or Santolík et al. [2010]). A shift in wave frequency can also be interpreted as a Doppler shift arising from a relative movement between source and observer, as reported by Inan et al. [2004]. Further ray tracing studies from Chum et al. [2009] and Breneman et al. [2009] achieve spectral shifts of individual chorus elements simply by wave dispersion along the ray path. These models were designed for explaining spectral differences seen on different spacecraft, assuming that they observe the same source. Even if our situation is different, i.e. one spacecraft observing two different sources, it demonstrates the influence of wave dispersion even along a rather short ray path (a few thousand kilometers) between the BWO–IR and the observer.

Acknowledgments. A. D. acknowledges support from the Russian Science Foundation under grant No.15-12-20005. U. T. and O. S. acknowledge support from the Praemium Academiae award and from the LH 15304 grant. The Editors thank Jim LaBelle and one anonymous reviewer for their help in evaluating this paper.

References

Agapitov, O., V. Krasnoselskikh, Yu. Zaliznyak, V. Angelopoulos, O. Le Contel, and G. Rolland, Observations and modeling of forward and reflected chorus waves captured by THEMIS, *Ann. Geophys.*, **29**, 541–550, 2011.

Angelopoulos, V., The THEMIS mission, *Space Sci. Rev.*, **141**, 1-4, 5–34, 2008.

Bonnell, J. W., F. S. Mozer, G. T. Delory, A. J. Hull, R. E. Ergun, C. M. Cully, V. Angelopoulos, and P. R. Harvey, The Electric Field Instrument (EFI) for THEMIS, *Space Sci. Rev.*, **141**, 1-4, 303–341, 2008.

Brice, N. M., An explanation of triggered very-low-frequency emissions, *J. Geophys. Res.*, **68**, 4626–4628, 1963.

Burton, R. K., and R. E. Holzer, The origin and propagation of chorus in the outer magnetosphere, *J. Geophys. Res.*, **79**, 7, 1014–1023, 1974.

Breneman, A. W., C. A. Kletzing, J. Pickett, J. Chum, and O. Santolík, Statistics of multispacecraft observations of chorus dispersion and source location, *J. Geophys. Res.*, **114**, A06202, 2009.

Chum, J., O. Santolík, D. A. Gurnett, and J. S. Pickett, Oblique lower band chorus waves: Time shifts between discrete elements observed by the Cluster spacecraft, *J. Geophys. Res.*, **114**, A00F02, 2009.

Demekhov, A. G., U. Taubenschuss, and O. Santolík, Simulation of VLF chorus emissions in the magnetosphere and comparison with THEMIS spacecraft data, *J. Geophys. Res.*, **122**, 166–184, 2017.

Inan, U. S., M. Platino, T. F. Bell, D. A. Gurnett, and J. S. Pickett, Cluster measurements of rapidly moving sources of ELF/VLF chorus, *J. Geophys. Res.*, **109**, A05214, 2004.

Johnson, H. R., Backward–wave oscillators, *Proc. IRE*, **43**, 6, 684–697, 1955.

Kennel, C. F., and H. E. Petschek, Limit on stably trapped particle fluxes, *J. Geophys. Res.*, **71**, 1, 1–28, 1966.

LeDocq, M. J., D. A. Gurnett, and G. B. Hospodarsky, Chorus source locations from VLF Poynting flux measurements with the Polar spacecraft, *Geophys. Res. Lett.*, **25**, 4063–4066, 1998.

Lepping, R. P., et al. (14 co-authors), The WIND Magnetic Field Investigation, *Space Sci. Rev.*, **71**, 1-4, 207–229, 1995.

Li, W., J. Bortnik, R. M. Thorne, C. M. Cully, L. Chen, V. Angelopoulos, Y. Nishimura, J. B. Tao, J. W. Bonnell, and O. Le Contel, Characteristics of the Poynting flux and wave normal vectors of whistler–mode waves observed on THEMIS, *J. Geophys. Res.*, **118**, 1461–1471, 2013.

Li, W., O. Santolík, J. Bortnik, R. M. Thorne, C. A. Kletzing, W. S. Kurth, and G. B. Hospodarsky, New chorus wave properties near the equator from Van Allen Probes wave observations, *Geophys. Res. Lett.*, **43**, 4725–4735, 2016.

Lin, R. P., et al. (19 co-authors), A three-dimensional plasma and energetic particle investigation for the Wind spacecraft, *Space Sci. Rev.*, **71**, 1-4, 125–153, 1995.

Lyubchich, A. A., A. G. Demekhov, E. E. Titova, and A. G. Yahnin, Amplitude–frequency characteristics of ion–cyclotron and whistler–mode waves from Van Allen Probes data, *Geomag. Aeron.*, **57**, 1, 40–50, 2017.

Macúšová, E., et al. (10 co-authors), Observations of the relationship between frequency sweep rates of chorus wave packets and plasma density, *J. Geophys. Res.*, **115**, A12257, 2010.

Matsui, H., K. W. Paulson, R. B. Torbert, H. E. Spence, C. A. Kletzing, W. S. Kurth, R. M. Skoug, B. A. Larsen, and A. W. Breneman, Nonlinearity in chorus waves during a geomagnetic storm on 1 November 2012, *J. Geophys. Res.*, **121**, 358–373, 2016.

McComas, D. J., S. J. Bame, P. Barker, W. C. Feldman, J. L. Phillips, P. Riley, and J. W. Griffee, Solar Wind Electron Proton Alpha Monitor (SWEPAM) for the Advanced Composition Explorer, *Space Sci. Rev.*, **86**, 563–612, 1998.

Meredith, N. P., R. B. Horne, A. Sicard–Piet, D. Boscher, K. H. Yearby, W. Li, and R. M. Thorne, Global model of lower band and upper band chorus from multiple satellite observations, *J. Geophys. Res.*, **117**, A10225, 2012.

Parrot, M., O. Santolík, D. Gurnett, J. S. Pickett, and N. Cornilleau–Wehrlin, Characteristics of magnetospherically reflected chorus waves observed by Cluster, *Ann. Geophys.*, **22**, 2597–2606, 2004.

Roux, A., O. Le Contel, C. Coillot, A. Bouabdellah, B. de La Porte, D. Alison, S. Ruocco, and M. C. Vassal, The search coil magnetometer for THEMIS, *Space Sci. Rev.*, **141**, 1-4, 265–275, 2008.

Santolík, O., M. Parrot, and F. Lefeuvre, Singular value decomposition methods for wave propagation analysis, *Radio Sci.*, **38**, 1, id.1010, 2003.

Santolík, O., D. A. Gurnett, J. S. Pickett, M. Parrot, and N. Cornilleau–Wehrlin, A microscopic and nanoscopic view of storm–time chorus on 31 March 2001, *Geophys. Res. Lett.*, **31**, L02801, 2004.

Santolík, O., D. A. Gurnett, J. S. Pickett, M. Parrot, and N. Cornilleau–Wehrlin, Central position of the source region of storm–time chorus, *Planet. Space Sci.*, **53**, 299–305, 2005.

Santolík, O., New results of investigations of whistler–mode chorus emissions, *Nonlin. Proc. Geophys.*, **15**, 4, 621–630, 2008.

Santolík, O., J. S. Pickett, D. A. Gurnett, J. D. Menietti, B. T. Tsurutani, and O. Verkhoglyadova, Survey of Poynting flux of whistler mode chorus in the outer zone, *J. Geophys. Res.*, **115**, A00F13, 2010.

Smith, C. W., J. L'Heureux, N. F. Ness, M. H. Acuña, L. F. Burlaga, and J. Scheifele, The ACE Magnetic Fields Experiment, *Space Sci. Rev.*, **86**, 613–632, 1998.

Taubenschuss, U., O. Santolík, H. Breuillard, W. Li, and O. Le Contel, Poynting vector and wave vector directions of equatorial chorus, *J. Geophys. Res.*, **121**, 11912–11928, 2016.

Taylor, W. W. L., and D. A. Gurnett, Morphology of VLF emissions observed with the Injun 3 satellite, *J. Geophys. Res.*, **73**, 17, 5615–5626, 1968.

Trakhtengerts, V. Y., Magnetosphere cyclotron maser: Backward wave oscillator generation regime, *J. Geophys. Res.*, **100**, A9, 17205–17210, 1995.

Trakhtengerts, V. Y., M. J. Rycroft, and A. G. Demekhov, Interrelation of noise–like and discrete ELF/VLF emissions generated by cyclotron interactions, *J. Geophys. Res.*, **101**, 13293–13302, 1996.

Trakhtengerts, V. Y., A. G. Demekhov, E. E. Titova, B. V. Kozelov, O. Santolik, D. A. Gurnett, and M. Parrot, Interpretation of Cluster data on chorus emissions using the backward wave oscillator model, *Phys. Plasmas*, **11**, 1345–1351, 2004.

Trakhtengerts, V. Y., A. G. Demekhov, E. E. Titova, B. V. Kozelov, O. Santolík, E. Macúšová, D. Gurnett, J. S. Pickett, M. J. Rycroft, and D. Nunn, Formation of VLF chorus frequency spectrum: Cluster data and comparison with the backward wave oscillator model, *Geophys. Res. Lett.*, **34**, L02104, 2007.

Tsyganenko, N. A., and M. I. Sitnov, Modeling the dynamics of the inner magnetosphere during strong geomagnetic storms, *J. Geophys. Res.*, **110**, A03208, 2005.

Yue, C., X. An, J. Bortnik, Q. Ma, W. Li, R. M. Thorne, G. D. Reeves, M. Gkioulidou, D. G. Mitchell, and C. A. Kletzing, The relationship between the macroscopic state of electrons and the properties of chorus waves observed by the Van Allen Probes, *Geophys. Res. Lett.*, **43**, 7804–7812, 2016.